The characteristics and structure of a transferred arcjet for dross-free plasma cutting

Sakuragi, Shunichi
Komatsu Ltd.

https://doi.org/10.15017/17354

出版情報：九州大学大学院総合理工学報告. 16 (4), pp.383-388, 1995-03-01. Interdisciplinary Graduate School of Engineering Sciences, Kyushu University
バージョン：
権利関係：

九州大学大学院総合理工学研究科報告
第16巻 第4号 383-388頁 平成7年3月

Engineering Sciences Reports, Kyushu University
(KYUSHU DAIGAKU SOGORIKOGAKU KENKYUKA HOKOKU)
Vol. 16, No. 4, pp. 383 - 388, March. 1995

The characteristics and structure of a transferred arcjet for dross-free plasma cutting

by
Shunichi SAKURAGI*

(Received November 3, 1994)

The flow condition of the transferred arcjet for the dross-free cutting in sheet-metal shape cutting is investigated with the spectroscopic technique. The electron density measurement shows that the two flow patterns exist depending on the flow rate that is a function of the discharge current. For the flow rate lower than the critical value, the flow is considered laminar, whereas for the higher flow rate, it is turbulent. It is also found from the cutting experiment that the dross-free cutting is obtained when the flow is laminar. The empirical formula for the dross-free cutting is suggested as a function of the specific energy of the arcjet.

1. Introduction

The sheet-metal shape cutting has been done mainly by two methods; one is the laser cutting and the other the plasma cutting. The former is applicable to the thin sheet-metal with high accuracy but the required cost is high. On the other hand, the latter can be used, so far, for the cutting of the thick sheet with lower cost. However its accuracy is low, because that the energy density of the arcjet is low and the kerf-width is large compared with the laser cutting. To obtain the better cut quality by the plasma cutting with lower cost, it is necessary to develop precision plasma cutting technology.

In the last decade, the intensive research on the characteristics of the transferred arcjet has been done to find a better way to stabilize and control its energy[1]. This effort has developed the precision plasma cutter with an oxygen plasma torch with small arc current (<50 A) and with nozzle diameters from 0.4 mm to 0.8 mm. Although the operating arc current of this torch is small, its energy density at the nozzle exit is extremely high and is comparable to that of a 1 kW CO_2 laser. Also, the accuracy and heat deformation are better than those obrained by the laser cutting.

The cut quality of the workpiece is greatly affected by the arcjet conditions, such as momentum, energy and temperature distributions in the arcjet. The analyses of the momentum and energy loss mechanisms in the transferred arcjet have been done by Sakuragi et al[2)3)]. Despite the intensive research on the characteristics of the transferred arcjet, the serious problem remains unsolved; the molten material recasts itself on the bottom of the cut edge and creates the hard-to-remove dross. Therefore, it is necessary to establish the method for the dross-free cutting.

*Komatsu Ltd.
**Communicated by Mitsuharu Masuda (Department of Energy Conversion Engineering)

The present paper discusses the arcjet conditions of the dross-free cutting. To clarify the structure of the arcjet for the dross-free cutting, the electron density distributions in the arcjet are measured for the wide range of the arc current and gas flow rate. These experiments indicate that the dross-free cutting condition depends on the arcjet structure, and the empirical formula for the dross-free cutting is suggested as a function of the specific energy of the arcjet.

2. Dross height of the plasma cutting

The schematic diagrams of the plasma cutting process and attached dross on the cut edge are shown in **Fig. 1**. To investigate the conditions of the dross-free cutting, the commercial plasma torch (Komatsu G940) is used.

To obtain the dross height, two carbon-steel plates are tested with the thickness of 3.2 mm and 6.0 mm. The results are shown in **Fig. 2 (a)** and **(b)**, where p_0 is the supply pressure in the gas reservoir, ϕ the exit diameter of the nozzle, I the arc current and D the stand-off distance between the nozzle exit and the test plate. This figure shows the dross height as a function of the cutting speed with various gas pressures. As shown in the figure, the dross in the low presure region differs greatly from that in the high pressure region. This suggests

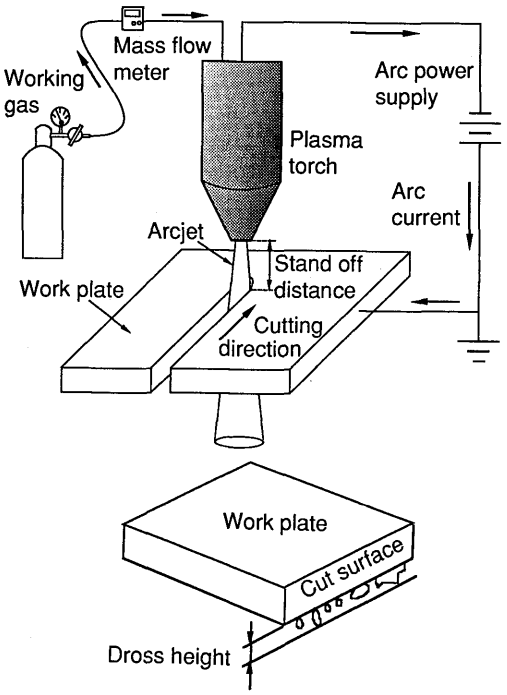

Fig. 1 Schematic diagrams of plasma cutting system and attached dross on the cut edge.

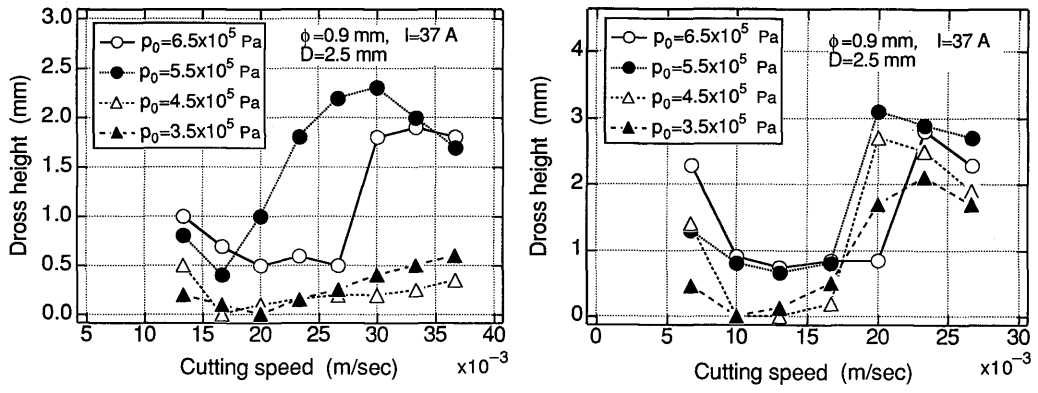

Fig. 2 Attached dross height as a function of cutting speed for (a) the plate thickness 3.2 mm and (b) the plate thickness 6.0 mm.

that the two flow patterns exist depending on the gas supply pressure.

3. Experimental setup and measurement principle

To clarify the detailed structure of the transferred arcjet for the dross-free curring, the electron number density n_e in the arcjet is measured with the commercial plasma torch (Komatsu G940) by the standard emission-based spectroscopy.

Figure 3 shows the schematic diagram of the experimental setup and the measuring instruments. The working gas is nitrogen. A small amount of hydrogen (~ 1% in volume) in added to measure the H_α spectral line (656.2 nm) whose value of FWHM (full-width at half-maximum) is used to determine the electron density. To calculate n_e, the tabulated values of n_e versus FWHM[4] were used. Under the assumption of LTE (local thermodynamic equilibrium), the temperatures in the arcjet are calculated from Saha's equation by assuming the pressure being atmospheric.

The coordinate system shown in **Fig. 4** is used to analyze the electron density from the measured intensity. This figure depicts the A-A′ cross-section of the arc column with radius R shown in **Fig. 3**, and x, y and z are the Cartesian coordinate, r the radial coordinate, respectively. The radiation intensity $I_\lambda(y)$ integrated along the line-of-sight (see **Fig. 4**) is written as

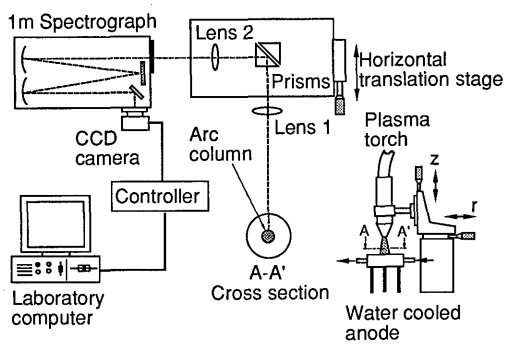

Fig. 3 Schematic diagram of experimental setup.

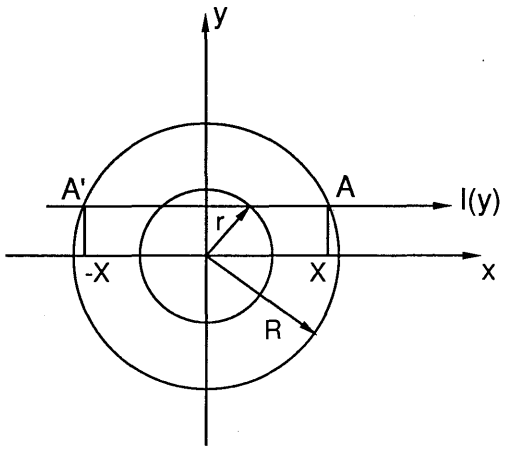

Fig. 4 Radiation intensity from a cylindrical arcjet.

$$I_\lambda(y) = 2\int_0^X \varepsilon_\lambda(r)\,dx = 2\int_y^R \frac{\varepsilon_\lambda(r)\,r\,dr}{\sqrt{r^2-y^2}} \tag{1}$$

To calculate n_e, the volume emission coefficient $\varepsilon_\lambda(r)$ should be known. By measuring $I_\lambda(y)$, the $\varepsilon_\lambda(r)$ can be obtained by the following Abel's inversion formula;

$$\varepsilon_\lambda(r) = -\frac{1}{\pi}\int_r^R \frac{\dfrac{dI_\lambda(y)}{dy}}{\sqrt{r^2-y^2}}\,dy \tag{2}$$

The above equation is integrated numerically by the trapezoidal rule. The accuracy was tested by integrating the known function, and was found to be ±3% for the ten points integration.

The spectral emission from the arc column is imaged onto the entrance slit of the 1 m Czerny-Turner spectrograph (see **Fig. 3**). The light is collimated by Lens 1 (f-number= 20, focal length=50 cm) and is imaged on the entrance slit through a double prism. This prism rotates the arc image 90° when focused by Lens 2 (focal length = 40 cm). The double prism and Lens 2 are mounted on a translation stage and the image is moved across the entrance slit along the axis of the arcjet column.

At the exit plane of the spectrograph, the light with a wavelength near the H_α transition is detected by the CCD camera having a 384×572 pixel array with a pixel size of 23 μm×23 μm. To avoid thermal noise, the detector is thermo-electrically cooled to −30 ℃ with the tap-water circulation. Data are taken at the several tens of the different points equaly spaced along the r-axis (from the center of the arcjet to the jet boundary), and are stored in the laboratory computer.

By moving the horizontal translation stage shown in **Fig. 3**, the focused image on the entrance slit are traversed along the z-axis from the nozzle exit to the anode surface.

4. Electron density in the arcjet

The electron density n_e along the jet center line was reported in the previous work[5], and it is not reproduced here. To detect the change of the flow pattern, the radial distribution of the electron density is measured under various operating conditions. **Figure 5** shows the results at $z=4.0$ mm with the gas flow rate as a parameter. The plasma torch has a nozzle with an exit diameter of 0.6 mm, and the discharge current is 12 A. This figure indicates that the critical flow rate exists, and the n_e-distribution differs greatly above and below this critical flow rate. For the lower flow rate, the two n_e-distributions agree very well. However, for the higher flow rate, the electron density is smaller than that for the lower flow rate, and fluctuates near the jet boundary. This result suggests that the flow changes from laminar to turbulent depending on the flow rate.

Figure 6 shows the relation between the arc current and the critical flow rate described above. To check the effect of the nozzle shape on the critical flow rate, similar measurements to **Fig. 5** were done with two nozzles having different diameter. The results of this experiment are shown in **Fig. 6**, and the data are found to be fit by the straight line passing through the origin. This means that the critical flow rate is proportional only to the discharge current.

5. Formulation of the dross-free condition

To investigate the relation between the dross-free condition and the flow transition, cutting tests with an oxygen plasma torch (Komatsu G940) are performed for the various arc current, gas flow rate and cutting speed. **Figure 7** shows the gas flow rate for the dross-free cutting as a function of the arc current. Since the dross-free condition depends on the cutting speed, these data are taken with the cutting speed that gives the best results. The broken line in **Fig. 7** is the critical flow rate, and the cut quality differs greatly above

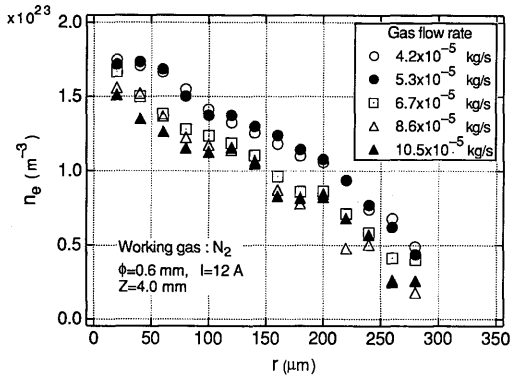

Fig. 5 Radial distributions of electron density at $z=4.0$ mm, for various gas flow rates.

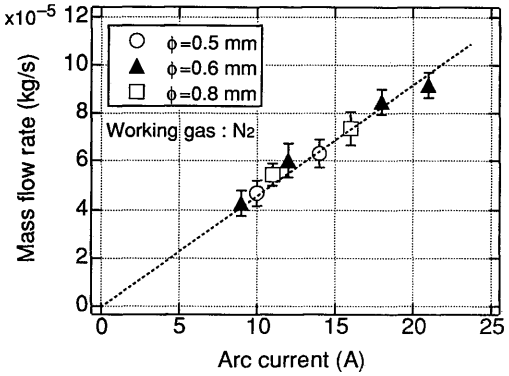

Fig. 6 Critical flow rate as a function of discharge current for various nozzle diameters.

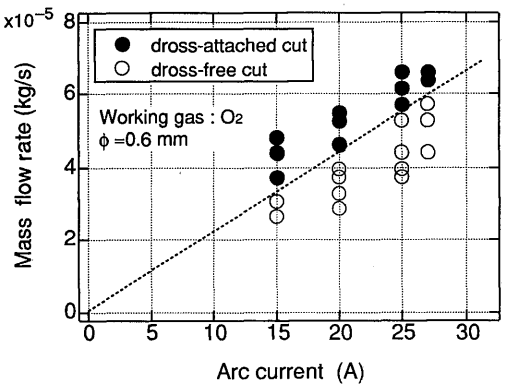

Fig. 7 Region of dross-free cutting expressed in terms of discharge current and mass flow rate of the working gas.

and below this line. This behavior is similar to that observed in **Fig. 6**, and it seems that the dross-free cutting is attained when the flow is laminar.

Figure 7 indicates that the dross-free condition is expressed as

$$\frac{I}{m} \gtrapprox 4.4\times10^5 \qquad \text{(A. s/kg)} \tag{3}$$

where m is the mass flow rate of the working gas and I the arc current. According to this formula, the dross-free cutting is obtained by the arc with high specific energy. However, the conventional plasma torch is unable to keep the stable arc in the dross-free condition, because the required flow rate for the swirl stabilization is insufficient for the dross-free condition, and the arc instability such as the double arcing is induced.

The present work strongly suggests the necessity of developing a new torch, the arc of

which is stabilized with the flow rate lower than the critical value for the stable dross-free cutting.

6. Conclusions

The flow condition of a transferred arcjet for the dross-free cutting is presented. The structure of the arcjet is obtained by the electron density measurement, and it is found that the flow changes from laminar to turbulent above the critical flow rate that is a function of the arc current. The cutting experiment shows that the dross-free cutting is attained for the flow rate lower than the critical value, where the flow is considered laminar and has much larger specific energy than that in the conventional torch. From the present work, it is found that the new torch should be developed for the stable dross-free cutting; the arc in this torch is stabilized by a swirl flow with the flow rate lower than the conventional torch.

References

1) Hypertherm Inc., "A History of Plasma Cutting (Milestones in the Development of a New Technology)", 1991.
2) Sakuragi, S., Cappelli, M. A., "An Analysis of Transferred Arcjet by Integral Method", Quarterly Journal of the Japan Welding Society, Vol. 10, No. 1, 1992, pp. 16-22 (in Japanese).
3) Sakuragi, S., Takashiri, M., "Investigation on Momentum Loss of Transferred Arcjet", Transactions of the Japan Society of Mechanical Engineers: B, Vol. 60, No. 573, 1994, pp. 112-118 (in Japanese).
4) Vidal, C. R., Cooper, J., and Smith, E. W., "Hydrogen Stark-Broadening Tables", The Astrophysical Journal Supplement Series, Vol. 25, No. 214, 1973, pp. 37-136.
5) Sakuragi, S., Inoue, M., and Cappelli, M. A., "Measurement of the Electron Number Density in a Transferred Arcjet Used for Plasma Cutting", Journal of High Temperature Society, Vol. 18, No. 1, 1992, pp. 27-35 (in Japanese).